

# Comparison of Local Nusselt Number Between Steady and Pulsating Jet at Different Jet Reynolds Number

<sup>1</sup>Rozli Zulkifli, <sup>1</sup>Kamaruzzaman Sopian, <sup>1</sup>Shahrir Abdullah and <sup>2</sup>Mohd Sobri Takriff

<sup>1</sup>Department of Mechanical and Materials Engineering

<sup>2</sup>Department Chemical and Process Engineering

Universiti Kebangsaan Malaysia, 43600 Bangi, Selangor  
MALAYSIA

rozli@eng.ukm.my <http://www.eng.ukm.my>

*Abstract:* - The study was carried out to determine the effect of pulsating frequencies exiting from a hot circular air jet on the local heat transfer of a flat impingement aluminium plate. The velocity profile of a steady heated circular air jet and pulsating air jet at frequencies of 10 and 20 Hz was measured in the first part of the study. The same set-up was used to measure the heat flux of the pulsating jet impinging on a flat aluminium plate. The heat flux of the heated air jet impinging on the plate was measured using a heat flux micro-sensor at radial positions between 0 to 12 cm away from the stagnation point. Measurement of the heat flux was used to calculate the local heat transfer coefficient and local Nusselt Number for steady air jet and for air jet pulsating frequencies of 10 and 20 Hz. The Reynolds number used were 16 000, 23 300 and 32 000. Results obtained show that the local Nusselt number calculated at all measurement point for pulsating jet were higher than the local Nusselt number for steady jet. The results for pulsating jet Nusselt number was higher than the steady jet Nusselt number for the value of frequencies measured are due to the higher localised heat transfer. The higher Nusselt number obtained at localized radial positions can be due to the higher instantaneous velocity as was shown from the velocity profile plotted in the first part of the experiment. The relationship between the two results shows that higher flow velocity and turbulence intensity gives higher localized heat transfer.

*Key-Words:* - Pulsating air jet, jet frequency, Nusselt number, Reynolds number, heat transfer coefficient

## 1 Introduction

Jets are widely used in industrial applications over a wide range of disciplines and configurations. Applications of impinging air jets include the cooling of electronic equipment, aircraft engine nacelle and blade, drying of textiles, annealing of metals and tempering of glass [1-2]. Unlike review articles by Martin [3] and Jambunathan [4] which discussed steady impingement in great detail, there are no similarly detailed review paper being published for pulsed jet impingement. The reasons why there is no study equivalent to the Martin [3] and Jambunathan [4] papers dealing with pulsed impingement heat transfer can be accorded to earlier findings regarding the effect of pulsation on heat transfer which have been conflicting due to many different factors. Among the earlier and widely referenced paper in pulsed jet impingement heat transfer is written out by Nevins & Ball [5]. Their tests on heat transfer between a flat plate and a pulsating jet showed that no significant heat transfer enhancement was obtained by using a pulsed air jet. The test was conducted at  $1200 < Re < 120\ 000$ ,  $10^{-4} < St < 10^{-2}$ , and nozzle to plate spacing between 8 to 32 nozzle diameters. Nevins & Ball [5] did not

document the extent of secondary flow structures in their experiments and since the experiment was studied at a very low Strouhal number this might affect their ability to demonstrate pulsed flow heat transfer enhancement. The application of pulse air jet was left dormant for many years due to this earlier finding and the difficulty of accurately controlling many pulse air jet parameters.

Recently, more researchers started to study experimentally and numerically the effect of flow pulsations on heat transfer enhancement. Sheriff & Zumbrunnen [6] investigated experimentally the effect of flow pulsation on cooling performance using arrays of jet. The presence of coherent structures was reported but no significant enhancement with respect to the heat transfer characteristics was recorded.

Kataoka & Suguro [7] show that stagnation point heat transfer for axisymmetric submerged jets is enhanced by the impingement of large-scale structures such as vortex rings on the boundary layer which occurred in pulse flow. Further tests carried out by Sailor et al. [8] on the effect of duty cycle variation on heat transfer enhancement for an impinging air jet showed significant heat transfer

enhancement. In this test, the effect of traditional variables such as jet to plate spacing, Reynolds number and pulse frequency were studied together with a new parameter, duty cycle representing the ratio of pulse cycle on time to total cycle time. Duty cycle was shown to have a significant effect on the heat transfer enhancement.

Mladin & Zumbrennen [9] investigated theoretically the influence of pulse shape, frequency and amplitude on instantaneous and time-averaged convective heat transfer in a planar stagnation region using a detailed boundary layer model. They reported that there exists a threshold Strouhal number,  $St > 0.26$  below which no significant heat transfer enhancement was obtained. Results obtained by Zumbrennen & Aziz [10] on the effect of flow intermittency on convective heat transfer to a planar water jet impinging on a constant heat flux surface reinforces this finding. This experiment carried out at  $St > 0.26$  found that local Nusselt number increases by up to 100%. However, Sailor et al. [8] used Strouhal number between 0.009 and 0.042 and still recorded significant enhancement in stagnation point heat transfer for pulse flow.

Azevedo et al. [11] investigated impingement heat transfer using a rotating cylinder valve for a range of pulse frequency. The results show that heat transfer degraded for all frequencies. In their experiments, velocity profile of the pulse jet shows the existence of a two-peak region for every flow cycle. This results in disturbance to the pulse flow and affects the flow structure and heat transfer. The dependence of pulse characteristics on convective heat transfer was discussed by Mladin & Zumbrennen [9].

In order to study the heat transfer characteristics of an impinging pulse air jet, the characteristics of a non-impinging pulse air jet needs to be initially understood. Farrington & Claunch [12] carried out a test to determine the influence of flow pulsations on the flow structures of an unforced planar jet with  $Re = 7200$  and  $0 < St < 0.324$ . The results of the test were captured using infrared imaging and smoke-wire visualization. They concluded that for pulsating jets, the vortices were larger than the steady jet and occurred closer to the nozzle. These larger vortices resulted in an increased entrainment and led to a wider angle of the potential core. Jets with large amplitude of pulsations entrained surrounding fluid more rapidly and decayed more quickly than steady jets. An increase in turbulence intensity can be associated with the pulse decay.

In pulsed flows, the size and formation of coherent structures are influenced by the amplitude

and frequency [13-14]. Large coherent flow structures can evolve from shear layers formed between a free jet flow and a surrounding fluid. The formation and interaction of flow structures can be influenced by the mixing within the boundary layer and a marked increase in turbulence intensities has been noted with pulse flows. Recent findings [8] on the enhancement of heat transfer due to pulse air jets have encouraged new research in this subject. Comprehensive data showing the effect of pulse frequency on local and average heat transfer profile are still limited and there is need of further investigation.

The only established applications of pulse air jet is in the industrial cleaning application in which pulse air jets are used for cleaning purposes. In the dry surface cleaning method, pulse air jets are used for the removal of fine particle. The effectiveness of pulse air jets in this application has been studied by Otani et. al. [15] and many other researchers [15]. Their findings have also supported the fact that consecutive pulse air jet is effective in the removal of fine particles due to the higher velocity and turbulence intensity.

The purpose of this study is to investigate steady and pulsating single circular jet heat transfer characteristics at three different Reynolds number. The focus of the study is given on the effect of flow pulsation frequencies at 10 and 20 Hz on the local heat transfer coefficient and local Nusselt number. Comparison between steady and pulsed jet heat transfer was discussed in details together with other published results. In this paper the stagnation point Nusselt number of a pulse jet means the time average value at the impingement point of the jet axis. The local Nusselt number of a pulse jet is the time average at a point on the impingement surface. The local Nusselt number is assumed to be radially symmetrical about the stagnation point. The average Nusselt number of a pulse jet is both a time average and an area average over the impingement surface. The total heat flux is proportional to the average Nusselt number.

## 2 Experimental Methods

### 2.1 Pulse flow system

Pulsating air jet was produced by repeatedly opening and closing nozzle exit at high repetition based on the desired pulsating frequency. There are a few ways in which a pulsating jet can be produced which includes the use of solenoid valve, self-excitation using a speaker and rotating valve such as

rotating ball valve or rotating cylinder valve. In order to achieve a mechanism which can produce high frequency pulse jet for a high pressurised air coming from a compressor, a system consisted of a rotating cylinder enclosed inside a block aluminium alloy body was chosen. The reason is due to:

- 1) robustness of the system in withstanding high pressure and high velocity of air coming from the compressor
- 2) high frequency pulsating jet can be produced depending on the maximum speed of the ac motor
- 3) variable nozzle exit can be used due to the requirement of the tests

Previously pulsating jet was mostly produce by a solenoid valve system. The opening and closing of the valve can be controlled depending on the applications requirement and the principle of the solenoid valve is given briefly here. In the energized state, an electrical current is sent to the solenoid coil on the valve. The current creates an electromagnetic force that lifts the solenoid plunger up into the solenoid coil. The lifting of the solenoid plunger opens an orifice that allows the fluid above the diaphragm to escape through the exhaust port and out through the outlet side of the valve. Fluid will escape from the chamber above the diaphragm more quickly than it can be replaced. This rapid loss of fluid causes the diaphragm to begin to lift. The diaphragm is forced to the full open position as the full underside of the diaphragm is exposed to the line pressure with the fluid above the diaphragm accelerated out. When the solenoid is de-energized, a small spring returns the plunger to a seated position. This closes off the flow of the fluid through the exhaust port. When the amount of fluid building up in the upper chamber increases, the diaphragm spring exerts a downward pressure and bring down the valve to a closed position. The system selected can produce pulsating jet at high frequency as compared to solenoid valve which can only produce jet with pulse frequency of upto 30 Hz while self-excitation jet using a speaker is only applicable for a low velocity laminar jet.

The pulse air jet is generated using a rotating cylinder valve driven by an electric motor which is controlled by an electronic motor controller. A 20 mm diameter hole was bored in the rotating cylinder normal to its axis to allow air passage. The aluminium alloy body is fixed to the supporting shaft and has a 40.2 mm hole diameter bored through its centre. The cylindrical rotating has a diameter of 40 mm and it was aligned inside the body such that a 0.1mm radial clearance is achieved between the stationary body and the cylindrical

valve. This is important in order to achieve a minimal leakage through the gap with the valve when it is in the closed position. The 15 mm diameter shafts at each end of the rotating valve were press-fits on sealed bearings to prevent air leakage through the shafts when the valve is closed. A 20 mm diameter hole was bored on each side of the aluminium block and the hole was aligned with the hole through the rotating cylinder. One end of the bored hole was connected to the compressed storage air tank and the other end was connected to the jet nozzle. In order to understand the principle of this system, it has to be visualized the moment after the air is supplied although the compressor. The compressor was started and the high air pressure is then released through the valve to the system, the rotating valve inside the stationary aluminium block will be rotated by the ac motor connected to it. Flow pulsation at the nozzle exit was achieved when the hole bored through the cylindrical rotating valve was aligned with the opposing holes in the valve body which is the hole for the incoming air and the hole for the nozzle. The frequency of the pulsating jet is dependent on the speed of the rotating cylindrical valve which is dependent also on the speed of the ac motor.

A jet nozzle of 20 mm diameter and length of 50 mm was selected for the whole of the tests configuration. A nozzle diameter of 20 mm was chosen because it was wide enough to give a jet exit profile of the flow with the use of the hot-wire anemometer. A radial flow velocity measurement of 14 point were taken at each 2 mm distance from the centre of the flow towards both side of the plate. This was done by moving the hot-wire using a vertical transverse system. A smaller nozzle diameter will not be able to give enough exit velocity profile at the same measurement distance and if the measurement distance is to be reduced to 0.5 mm, errors associated with the measurement will be increased. Figure 1 show an assembly diagram of the rotating valve pulse jet system.

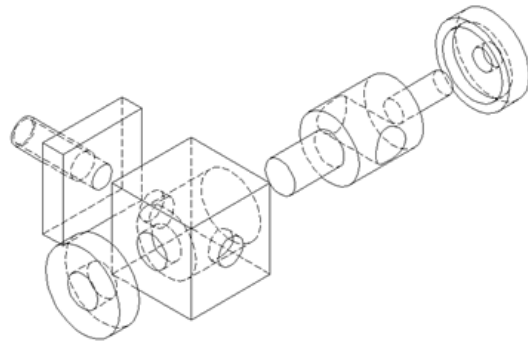


Fig. 1 An assembly diagram of pulse jet system.

Figure 2 shows the schematic diagram of the experimental test set-up. The pressurised air used in the experiment is supplied through the compressor. The air is continuously fed through a permanent piping to the heating chamber and the nozzle. The supply pipe of the air storage compressor tank is controlled by a stop valve. A pressure regulator

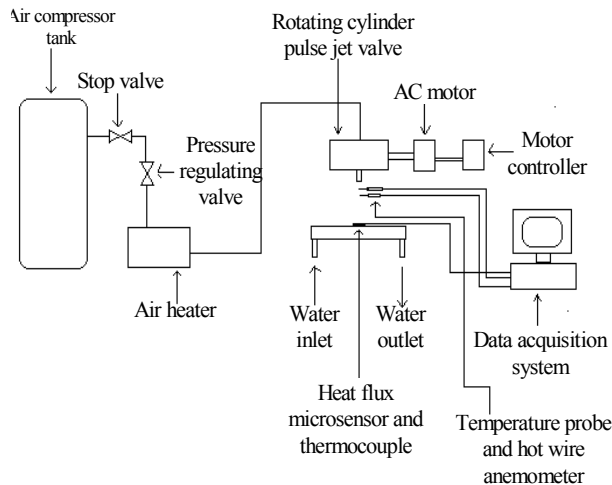


Fig. 2 Schematic diagram of the experimental test set-up.

was placed in between the air heater and the stop valve to regulate the supply of air. An air heater is used to heat the air jet with an associated maximum air temperature of 60°C.

## 2.2 Heat transfer measurement

Hot-wire sensors were used in constant-temperature mode to measure velocity of the pulsating jet. Hot-wire anemometer used in this experimental set-up is model 54T36 mini-CTA from Dantec Dynamics, Inc. Straight probes type 55P16 are mounted on a probe holder with the probe axis parallel with the dominant velocity direction. The sensor wires are made of etched tungsten wire of 5  $\mu\text{m}$  diameter and approximately 1.2 mm in length with length to diameter ratio of 240. The probe is mounted in a probe support which is equipped with a cable and BNC connector, one for each sensor on the probe. The probe bodies and the probe support are designed so that their outer surfaces are electrically insulated from the electrical circuitry of the probe or anemometer circuit. They can therefore be mounted directly to any metal part of the test rig without the risk of ground loops. The distance between the

probe and the miniCTA is kept as small as possible. The standard cable length used is 4 meters probe cable plus 1 meter support cable. The traverse system is used to move the probe around in the flow. The anemometer selected for use in this setup is made by Dantec Dynamics, Inc which includes 4 channels probe connections. The anemometer set-up consists of CTA hardware set-up and Signal conditioner filter and gain adjustment.

In order to obtain a velocity profile of a steady and pulsating jet exiting the nozzle, a hot-wire anemometer was used. Before the experiment can start, the hot-wire anemometer is configured, the software system initialized and the calibration process has been completed according to the method discussed earlier. After the calibration of the hot-wire probe, the system is ready to be used for jet flow profile measurement. Time-averaged velocity of the centreline jet exit air close to the nozzle was measured by placing the hot-wire probe at selected locations. Figure 3 shows the set-up for the mini-CTA Hot-wire anemometer by DANTEC DYNAMICS and the position of the hot-wire probe at centreline of the flow 2 mm from the nozzle exit leading edge..

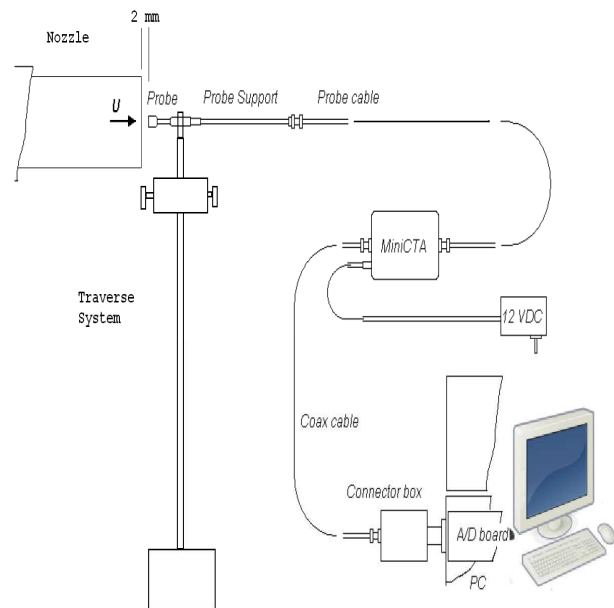


Fig. 3 Schematic diagram of the mini-CTA set-up and the position of hot-wire probe for radial velocity measurement at 2 mm from the nozzle.

The heat flux of the heated air jet impinging on the plate was measured using a heat flow and integral thermocouple sensor from RdF Corporation.

Calibration information and related measurement uncertainties for the sensor was provided by the manufacturer. The sensor is bonded on the plate by a laminating adhesive and is located at the centre of the plate. The impingement plate surface was covered by a Kapton sheet having the same thermal conductivity as the heat flux sensor so that the presence of the sensor would not alter the temperature distribution. The sensor provided voltage outputs corresponding to heat flux and plate temperature.

Heat transfer measurements were recorded from a heat flux micro-sensor bonded on the water-cooled aluminium block as shown in Figure 4. The impingement block was constructed from two 12 mm thick, 300 mm by 300 mm wide aluminium plates. Both plates were milled to a depth of 10 mm so that only a 2 mm thick wall between the impingement area and the water passage remained. The plates were bonded to each other to create a water-tight aluminium block. Three 12 mm connecting nozzles were attached to the lower part on the rear of the block to allow the cooling water in and another three on the upper part to allow the discharge of the water. Two K-type thermocouples were attached on the rear of the plate at a distance 120 mm apart to monitor the plate temperature. The plate was maintained at a temperature of 20°C throughout each of the tests.

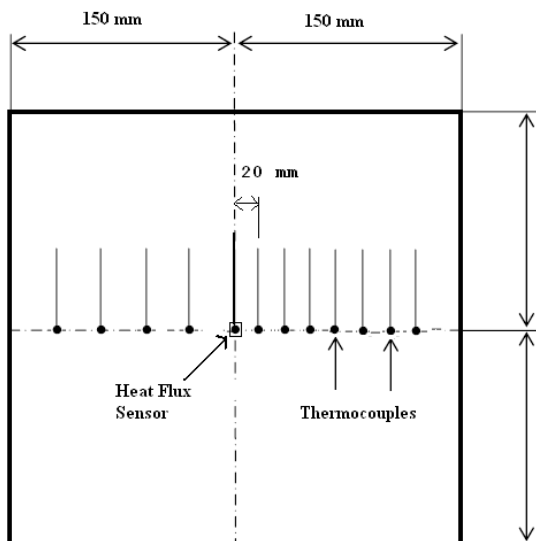


Fig. 4 The locations of the thermocouples and heat flux sensor on the flat impingement surface.

Data acquisition system was used to record the temperature and heat flux measurements from the thermocouples and heat flux sensor into a computer

for data processing and analysis. Data acquisition module used in this set-up is an ADC (analogue-to-digital converter). An ADC was used to convert analogue thermocouples signal into 16-bit digital signal. The data acquisition module used was "ADAM-4019+" made by Advantech Company Limited. The ADAM-4019+ is a 16-bit, 8-channel thermocouple analog input module that provides programmable input ranges on all channels. The ADAM-4019+ uses a 16-bit microprocessor-controlled sigma-delta A/D converter to convert sensor voltage or current into digital data. The digital data is then translated into engineering units. When prompted by the host computer, the module sends the data to the host through a standard RS-485 interface. The module supported eight input ports for thermocouples (six differential ports and two single-ended ports). It was suitable for connecting different types of thermocouples (ie. J, K, T, E, R, S and B types) with mV, V and mA input signals. The sampling rate for each channel was set at 1000 samples per second and the accuracy was  $\pm 0.1\%$  of the input voltages. The module is using regulated DC power supply from +10 VDC to +30VDC and the power consumption was 0.8 watts per each module.

The values of heat flux and plate temperature for the stagnation point and local measurements at different radial positions were monitored and recorded by the data acquisition system. Local heat transfer measurements were recorded at radial distances from 0-12 mm from the stagnation point. The instantaneous Nusselt number was calculated using the following equation:

$$Nu = \frac{q'' D}{(T_j - T_w) k} \quad (1)$$

where  $q''$  is the stagnation point heat flux measured by the sensor,  $D$  is the nozzle diameter,  $k$  is the thermal conductivity of the air jet evaluated at film temperature,  $T_j$  is the temperature of the hot air jet and  $T_w$  is the temperature of the plate at the stagnation point. The average Nusselt number based on the local temperature difference was calculated by numerically integrating the heat flux measurement over the impingement area.

### 3 Results and Discussion

Table 1 shows the values of the parameters that were investigated. The value the local heat transfer coefficient and local Nusselt numbers are

considered to be functions of Reynolds number and radial distance from the stagnation point. Duty cycle and  $x/D$  were not varied in this experiment.

Table 1: Parameters investigated in the experiments

Parameter	Values
Re	16000, 23000, 32000
St	$0.008 < St < 0.123$
$x/D$	4
DC	33%
D	20 mm
F	10-80Hz

To confirm the accuracy of the present work, the value of the steady jet Nusselt number versus Reynolds number was plotted and compared to the results of several previous researchers work as reported by Jambunathan et al. [4]. Figure 5 shows that the measured Nusselt numbers for the steady jet are comparable with previous experiments.

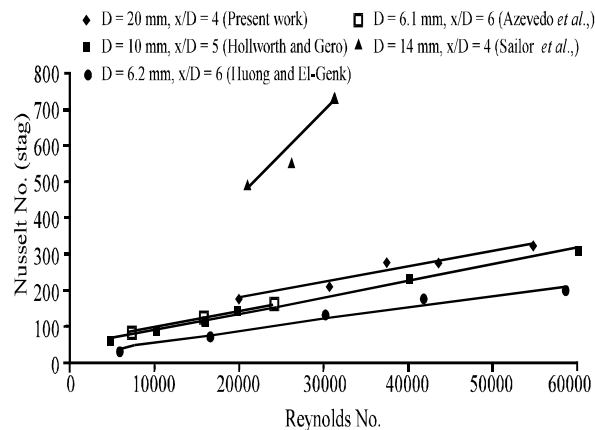


Fig. 5 Comparison of steady flow stagnation point Nusselt number.

The steady Nusselt number values obtained by Sailor et al. [8] were higher than those documented by other research work. Their calculations of Nusselt numbers were based on the difference of temperature between the stagnation point and the local adiabatic wall temperature. The average air temperature at the stagnation point is lower than the air temperature at the jet nozzle because ambient cool air is entrained in the pulse jet. This explains why Sailor et al.[8] recorded a higher value of Nusselt number for the same test parameters.

Figure 6 shows the variation of stagnation point and average Nusselt number with Reynolds number at nozzle to plate spacing,  $x/D$  equal to 4 for

frequencies from 20-80 Hz. Stagnation Nusselt number increases with higher Reynolds numbers as predicted.

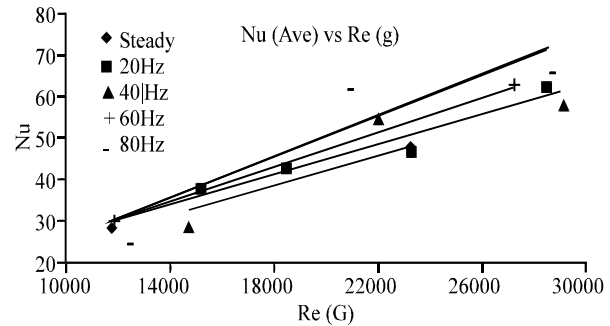


Fig. 6 Variation of stagnation point and average nusselt number with Reynolds number,  $Re(G)$  at nozzle to plate spacing,  $x/D = 4$  for frequencies from 20-80 Hz.

Table 2-4 show the local parameters of heat flux, plate temperature, heat transfer coefficient and Nusselt number for steady jet and jet at frequency of 10 Hz and 20 Hz for Reynolds number of 16000. Figure 7 and 8 show a graph of local Nusselt number against radial distance ratio for frequencies of 10Hz and 20Hz for Reynolds number of 16000. Radial distance ratio is the ratio of the radial distance over the diameter of the nozzle. The graph shows that the local Nusselt numbers for pulsating flow at stagnation point is higher for steady air jet. At radial distance ratio of 1, local Nusselt number are comparable for both steady and pulsating jet. However, further away from stagnation point, at radial distance ratio between 2 and 6, local Nusselt number for both 10 and 20 Hz pulsating jet are higher than for steady jet. The increases in local Nusselt number are between 15.7-166% for pulsating jet at frequency of 10 Hz. Eventhough the highest enhancement is 166% for radial distance ratio of 6, the value of local Nusselt number is too low to contribute significantly towards the total average Nusselt number.

Table 5-7 show the local parameters of heat flux, plate temperature, heat transfer coefficient and Nusselt number for steady jet and jet at frequency of 10 Hz and 20 Hz for Reynolds number of 23300. Figure 9 and 10 show a graph of local Nusselt number against radial distance ratio for frequencies of 10Hz and 20Hz for Reynolds number of 16000.

Table 2. Local Parameters at Radial distance between 0 to 12 cm from stagnation point for steady at Reynolds number of 16000.

Radial distance (cm)	Local Heat Flux, q (W/m <sup>2</sup> )	Local Temp (°C)	Local Heat Transfer Coeff. (W/m <sup>2</sup> .K)	Local Nusselt Number
0	7400.0	27	194.7	155.8
2	6200.0	24.4	152.5	122.0
4	3889.5	20.2	86.7	69.4
6	2142.1	17.2	44.8	35.8
8	1078.9	14.7	21.5	17.2
10	500.0	13.2	9.7	7.7
12	231.6	12.5	4.4	3.5

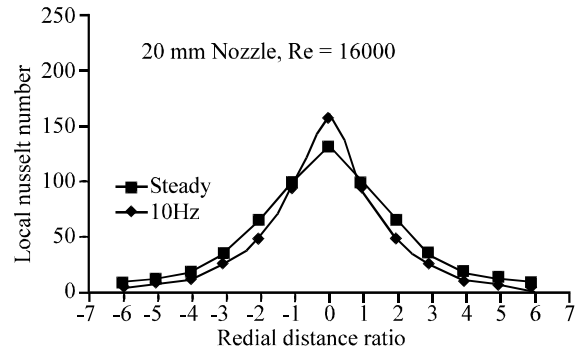


Fig. 7 Comparison between local Nusselt numbers of steady and pulsating jet of 10 Hz for Reynolds number = 16000.

Table 3. Local Parameters at Radial distance between 0 to 12 cm from stagnation point for pulsating jet frequency of 10 Hz at Reynolds number of 16000.

Radial distance (cm)	Local Heat Flux, q (W/m <sup>2</sup> )	Local Temp (°C)	Local Heat Transfer Coeff. (W/m <sup>2</sup> .K)	Local Nusselt Number
0	6473.7	25.3	163.1	130.5
2	5810.5	24.1	141.9	113.5
4	4378.9	21.4	100.4	80.3
6	2842.1	18.1	60.6	48.5
8	1563.2	15.6	31.6	25.3
10	905.3	14.1	17.8	14.2
12	605.3	13	11.6	9.3

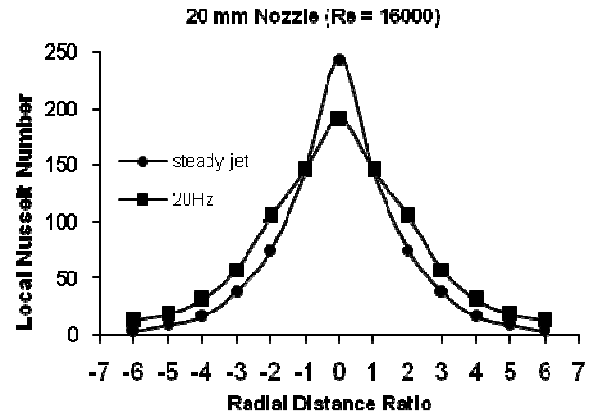


Fig. 8 Comparison between local Nusselt numbers of steady and pulsating jet of 20 Hz for Reynolds number = 16000.

Table 4. Local Parameters at Radial distance between 0 to 12 cm from stagnation point for pulsating jet frequency of 20 Hz at Reynolds number of 16000.

Radial distance (cm)	Local Heat Flux, q (W/m <sup>2</sup> )	Local Temp (°C)	Local Heat Transfer Coeff. (W/m <sup>2</sup> .K)	Local Nusselt Number
0	6010.5	25.5	152.2	121.7
2	5452.6	24.2	133.6	106.9
4	4336.8	21.4	99.5	79.6
6	2984.2	18.5	64.1	51.3
8	1715.8	16.2	35.1	28.1
10	989.5	14.6	19.6	15.7
12	636.8	13.6	12.4	9.9

Table 5. Local Parameters at Radial distance between 0 to 12 cm from stagnation point for steady at Reynolds number of 23300.

Radial distance (cm)	Local Heat Flux, q (W/m <sup>2</sup> )	Local Temp (°C)	Local Heat Transfer Coeff. (W/m <sup>2</sup> .K)	Local Nusselt Number
0	8894.7	28.9	246.4	197.1
2	7610.5	26.1	195.6	156.5
4	5078.9	21.8	117.6	94.1
6	2963.2	18.2	63.3	50.6
8	1536.8	15.2	30.9	24.7
10	763.2	13.6	14.8	11.9
12	410.5	12.4	7.8	6.2

Table 6. Local Parameters at Radial distance between 0 to 12 cm from stagnation point for pulsating jet frequency of 10 Hz at Reynolds number of 23300.

Radial distance (cm)	Local Heat Flux, q (W/m <sup>2</sup> )	Local Temp (°C)	Local Heat Transfer Coeff. (W/m <sup>2</sup> .K)	Local Nusselt Number
0	8168.4	29.5	230.1	184.1
2	7568.4	27.6	202.1	161.7
4	5947.4	24.0	144.9	115.9
6	3905.3	20.7	88.1	70.4
8	2315.8	17.4	48.7	38.9
10	1421.1	15.2	28.5	22.8
12	947.4	14.2	18.6	14.9

Table 7. Local Parameters at Radial distance between 0 to 12 cm from stagnation point for pulsating jet frequency of 20 Hz at Reynolds number of 23300.

Radial distance (cm)	Local Heat Flux, q (W/m <sup>2</sup> )	Local Temp (°C)	Local Heat Transfer Coeff. (W/m <sup>2</sup> .K)	Local Nusselt Number
0	6989.5	28.4	191.0	152.8
2	6484.2	27.0	170.4	136.3
4	5047.4	23.9	122.8	98.2
6	3368.4	20.5	75.6	60.5
8	2042.1	17.7	43.2	34.5
10	1194.7	16.1	24.4	19.5
12	742.1	15.0	14.8	11.9

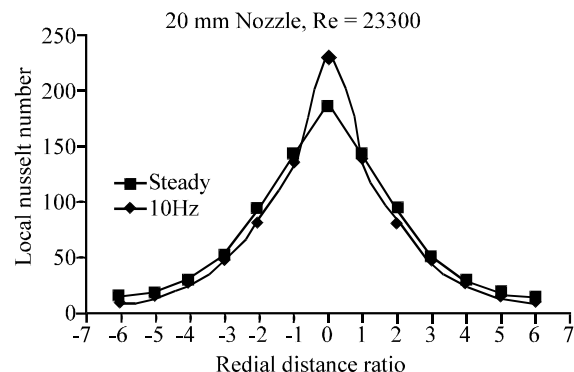


Fig. 9 Comparison between local Nusselt numbers of steady and pulsating jet of 10 Hz for Reynolds number = 23300.

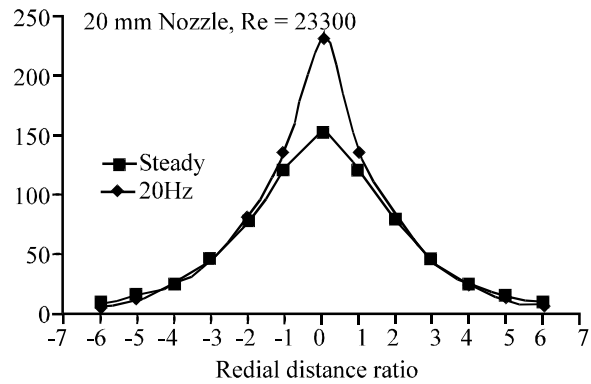


Fig. 10 Comparison between local Nusselt numbers of steady and pulsating jet of 20 Hz for Reynolds number = 23300.

At Reynolds number of 23300, stagnation point heat transfer is higher at steady jet compared to pulsating jet at frequencies of 10 and 20 Hz. At radial distance ratio of 2-6, pulsating jet at frequency 10 Hz shows an increase from 23.3% at radial distance ratio 2 (40 mm from stagnation point) to 140.3% at radial distance ratio 6 (120 mm from stagnation point). For jet frequency 20 Hz, pulsating jet only shows heat transfer increases between 19-99% between radial distance 3 and 6. However, this increases does not give potential impact on the overall heat transfer value.

Table 8 to 10 show the local parameters of heat flux, plate temperature, heat transfer coefficient and Nusselt number for steady jet and jet at frequency of 10 Hz and 20 Hz for highest Reynolds number of 32000. Figure 9 and 10 show a graph of local Nusselt number against radial distance ratio for frequencies of 10 Hz and 20 Hz for Reynolds number of 32000.

At pulsating frequency of 10 Hz, heat transfer at all radial distance ratio show higher heat transfer value than steady jet. Higher turbulence intensity at these positions is believed to contribute to the increase in heat transfer. The higher turbulence obtained could be due to the higher localized instantaneous velocity as recorded earlier. The average Nusselt numbers for the pulse jet is higher than the steady jet tested by at least 30%.

The present results show that the average heat transfer on the impingement area is enhanced quite significantly even though the stagnation point heat transfer decreases. These increases are shown to be available for a system that uses a single pulse jet impinging on an area with radius up to 6 times the nozzle diameter. The results show that higher mass flow rate will also influence the heat transfer

measurements. Graph for pulsating frequency of 20 Hz also showing a heat transfer increase at all radial distance except at stagnation point. Results from all three different Reynolds number show that higher Reynolds number will give higher Nusselt number for pulsating jet at 10 and 20 Hz. The average Nusselt number is higher for pulsating jet compared to steady jet at Reynolds number of 32000. At Reynolds number of 16000 and 23300, only local Nusselt number at radial distance ratio of 3 and above will give a heat transfer enhancement. However, these enhancement is not enough to compensate a lower stagnation point heat transfer value as compared to higher steady jet stagnation point heat transfer.

Table 8. Local Parameters at Radial distance between 0 to 12 cm from stagnation point for steady at Reynolds number of 32000.

Radial distance (cm)	Local Heat Flux, q (W/m <sup>2</sup> )	Local Temp (°C)	Local Heat Transfer Coeff. (W/m <sup>2</sup> .K)	Local Nusselt Number
0	9747.4	31.3	289.2	231.4
2	8242.1	28.1	223.4	178.7
4	5573.7	23.1	133.0	106.4
6	3500.0	19.2	76.4	61.1
8	2010.5	16.1	41.1	32.9
10	1068.4	14.1	21.0	16.8
12	531.6	12.6	10.1	8.1

Table 9. Local Parameters at Radial distance between 0 to 12 cm from stagnation point for pulsating jet frequency of 10 Hz at Reynolds number of 32000.

Radial distance (cm)	Local Heat Flux, q (W/m <sup>2</sup> )	Local Temp (°C)	Local Heat Transfer Coeff. (W/m <sup>2</sup> .K)	Local Nusselt Number
0	9263.2	32.9	288.6	230.9
2	8878.9	31.0	261.1	208.9
4	7168.4	27.0	188.4	150.7
6	4747.4	22.8	112.4	89.9
8	2926.3	19.4	64.1	51.3
10	1736.8	17.1	36.2	29.0
12	1210.5	15.7	24.5	19.6

Table 10. Local Parameters at Radial distance between 0 to 12 cm from stagnation point for pulsating jet frequency of 20 Hz at Reynolds number of 32000.

Radial distance (cm)	Local Heat Flux, q (W/m <sup>2</sup> )	Local Temp (°C)	Local Heat Transfer Coeff. (W/m <sup>2</sup> .K)	Local Nusselt Number
0	8831.6	30.5	256.0	204.8
2	8363.2	29.1	232.6	186.1
4	6663.2	25.7	169.5	135.6
6	4384.2	21.7	101.3	81.0
8	2594.7	18.5	55.8	44.6
10	1584.2	16.6	32.7	26.2
12	1131.6	15.2	22.7	18.2

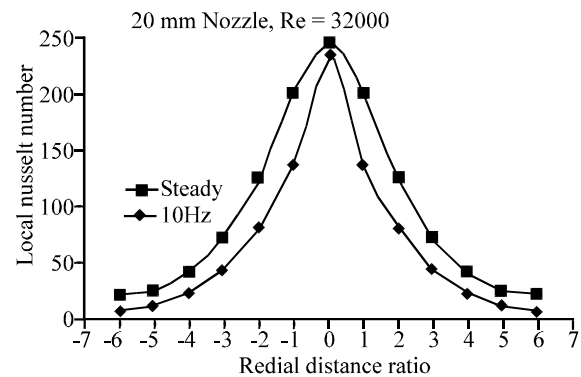


Fig. 9 Variation of local Nusselt numbers with radial distance at frequencies of 10 Hz for Reynolds number 32000.

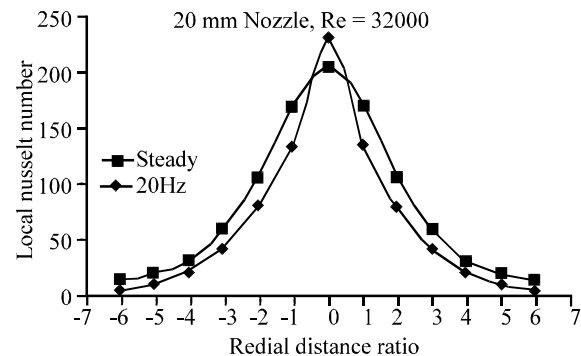


Fig. 10 Variation of local Nusselt numbers with radial distance at frequencies of 20 Hz for Reynolds number 32000.

## 4 Conclusion

The results of the experiments show that there is significant enhancement in the local heat transfer of the pulse flow at positions of radial distance 3-6 for pulsating frequencies 10 and 20 Hz at Reynolds number of 16000 and 23300. The stagnation point heat transfer does not show any enhancement for the three Reynolds numbers investigated. The average Nusselt number for the pulse jet is for both frequencies investigated at Reynolds number 32000. The degree of enhancement is in the range of 30%. Heat transfer in the pulse flow mode is complex and dependent on the flow structure of the jet. The significant enhancement of the heat transfer at local distances away from the stagnation point resulted in higher average Nusselt numbers for pulse flow compared to steady flow at these localized point. Significant turbulence intensity caused by pulsating the jet resulted in the increase recorded. The degradation in heat transfer at the stagnation point for pulsating jet is believed to be due to the distribution of velocity over a larger radial distance.

### References:

- [1] Chaniotis, A.K., Poulikakos, D. & Ventikos, Y. 2003. Dual pulsating or steady slot jet cooling of a constant heat flux surface. *Journal of Heat Transfer*, 125(4): 575-586.
- [2] Kondjoyan, A., Peneau, F. & Boisson, H.C. 2002. Effect of high free stream turbulence on heat transfer between plates and air flows: a review of existing experimental results. *Int. Journal of Thermal Sciences*, 41: 1-16.
- [3] Martin, H. 1977. Heat and mass transfer between impinging gas jets and solid surfaces. In: *Advances in heat transfer*. New York, Academic Press, Inc., 13: 1-60.
- [4] Jambunathan, K., Lai, E., Moss, M.A. & Button, B.L. 1992. A review of heat transfer data for single circular jet impingement. *Int. J. of Heat and Fluid Flow*, 13(2): 106-115.
- [5] Nevin, R.G. & Ball, H.D. 1961. heat transfer between a flat plate and a pulsating impinging jet. National Heat Transfer Conference, Boulder, CO. ASME.
- [6] Sheriff, H.S. & Zumbrennen, D.A. 1994. Effect of flow pulsations on the cooling effectiveness of an impinging jet. *Journal of Heat Transfer*, 116(4): 886-895.
- [7] Kataoka, K. & Suguro, M. 1987. The effect of surface renewal due to large scale eddies on jet impingement heat transfer. *Int. Journal of Heat and Mass Transfer*, 30(3): 559-567.
- [8] Sailor, D.J., Rohli, D.J. & Fu, Q. 1999. Effect of variable duty cycle flow pulsations on heat transfer enhancement for an impinging air jet. *Int. Journal of Heat and Fluid Flow*, 20(6): 574-580.
- [9] Mladin, E.C. & Zumbrennen, D.A. 2000. Alterations to coherent flow structures and heat transfer due to pulsations in an impinging air-jet. *Int. Journal of Thermal Sciences*, 39(2): 236-248.
- [10] Zumbrennen, D.A. & Aziz, M. 1993. Convective heat transfer enhancement due to intermittency in an impinging jet. *Journal of Heat Transfer*, 115(1): 91-98.
- [11] Azevedo, L.F.A., Webb, B.W. & Queiroz, M. 1994. Pulsed air jet impingement heat transfer. *Experimental Thermal and Fluid Science*, 8: 206-213.
- [12] Farrington, R.B. & Claunch, S.D. 1994. Infrared imaging of large amplitude, low frequency disturbances on a planar jet. *AIAA Journal*, 32: 317-323.
- [13] Mladin, E.C. & Zumbrennen, D.A. 1995. Dependence of heat transfer to a pulsating stagnation flow on pulse characteristics. *Journal of Thermophysics and Heat Transfer*, 9(1): 181-192.
- [14] Otani, Y., Norikazu, N. & Emi, H. 1995. Removal of fine particles from smooth flat surfaces by consecutive pulse air jets. *Aerosol Science and Technology*, 23: 665-673.
- [15] Lu, H.C. & Tsai, C.J. 1999. Influence of design and operation parameters on bag-cleaning performance of pulse-jet baghouse. *Journal of Environmental Eng.*, 125(6): 583-591.